Journal of Solid State Chemistry **156,** 452–457 (2001)
doi:10.1006/jssc.2000.9022, available online at http://www.idealibrary.com on IDEAL®

Magnetic Properties of $LnTi_{0.5}V_{0.5}O_3$ (Ln = Ce and Pr)

K. Yoshii and H. Abe*

Synchrotron Radiation Research Center, Japan Atomic Energy Research Institute (JAERI), Mikazuki, Hyogo 679-5148, Japan; and
**National Research Institute for Metals (NRIM), Sengen, Tsukuba, Ibaraki 305-0047, Japan*

Received June 24, 2000; in revised form October 13, 2000; accepted November 6, 2000; published online December 21, 2000

Magnetic properties of $LnTi_{0.5}V_{0.5}O_3$ (Ln = Ce and Pr), which are solid solutions between the perovskites $LnTiO_3$ and $LnVO_3$, have been investigated. Their crystal structures are an orthorhombic perovskite type (*Pnma*), where the Ti and V ions are settled with random occupation at the same crystallographic site. DC susceptibility–temperature (χ–T) curves exhibit magnetic transitions at $T_N \sim 50$ K. These temperatures are considerably lower than those of the end compounds $\sim$116–145 K. The deviation between FC (field-cooled) and ZFC (zero-field-cooled) curves, and the susceptibility cusps only in the ZFC curves are also observed below $T_{N2} \sim 30$ K. Magnetization at 6 K changes almost linearly with logarithm of time. AC susceptibility–temperature ($\chi(\nu)$–T) curves show the maximums of both real and imaginary parts of $\chi(\nu)$. The susceptibility maximum temperatures exhibit temperature dependence. These magnetic properties suggest the formation of spin-glasses, arising from the random occupation of the Ti and V ions. © 2001 Academic Press

Key Words: **perovskite; titanate; vanadate; canted-antiferromagnetism; spin-glass.**

INTRODUCTION

The perovskite-type oxides $LnTiO_3$ and $LnVO_3$ (Ln: lanthanides) have an orthorhombic perovskite structure (space group *Pnma*; $GdFeO_3$ type) (1–9). Because of strong Coulomb repulsion between the Ti3d and V3d electrons, these systems are regarded as Mott–Hubbard-type insulators having localized Ti^{3+} ($3d^1$; $S = \frac{1}{2}$) and V^{3+} ($3d^2$; $S = 1$) moments. For the $LnTiO_3$ systems with Ln = La–Sm, and all the $LnVO_3$ systems, the moments order magnetically with Neel temperatures (T_N) between $\sim$140 and $\sim$50 K. This order is accompanied by the spin canting of the moments due to the antisymmetric Dzyaloshinsky–Moriya interaction. Therefore it is denoted as canted antiferromagnetism.

The transitions for $CeTiO_3$ and $PrTiO_3$ occur at $T_N \sim 116$–120 K and $\sim$96–120 K, respectively (1–7). Their susceptibility–temperature curves show other transitions at low temperatures ($\sim$ 60–80 K). They are brought about by the order of magnetic moments of Ce^{3+} ($4f^1$) and Pr^{3+} ($4f^2$), owing to the internal magnetic field from Ti^{3+}. The transition temperatures of $CeVO_3$ and $PrVO_3$ are $T_N \sim 130$–140 K (8). Detailed magnetic properties have been investigated for $CeVO_3$ (8), where a first-order magnetostrictive distortion occurs slightly below T_N due to the coorporative Jahn–Teller distortion. This phenomenon causes anomalous properties such as a reversal of the direction of V^{3+} moments.

The physical properties of these compounds have been extensively studied in this decade. To investigate further variations in their physical properties, we have prepared the solid solution systems $LnTi_{0.5}V_{0.5}O_3$ with Ln = Ce and Pr and studied their magnetic properties in this work. The properties for such solid solutions have been reported mainly for the systems containing the 3d transition metals of Mn–Cu (10, 11).

EXPERIMENTAL PROCEDURES

The samples were prepared by the solid-state reaction method according the reactions:

$$CeO_2 + (\tfrac{1}{2})\,TiO + (\tfrac{1}{2})\,VO \rightarrow CeTi_{0.5}V_{0.5}O_3, \text{ and}$$

$$(\tfrac{1}{2})\,Pr_2O_3 + (\tfrac{1}{4})\,Ti_2O_3 + (\tfrac{1}{4})\,V_2O_3 \rightarrow PrTi_{0.5}V_{0.5}O_3.$$

The purity of the starting materials was 4N–3N (Soekawa). As Ce_2O_3 is unstable, CeO_2 was used. The initial mixtures were ground, pelletized, fired at $\sim$1550°C in vacuum better than 10^{-4} Pa for 24 h, and cooled down to room temperature with the cooling rates of $\sim$400–600°C/h. The firing was repeated for two to three times with intermediate grindings. For comparison, the end compounds were also prepared in the same manner. Each sample was prepared twice at least, and was verified to show reproducible structural and magnetic properties.

The compositions determined from both thermogravimetry and atomic absorption were $LnTi_{0.47\text{–}0.50(2)}V_{0.47\text{–}0.51}O_{3+\delta}$ with $\delta = 0.020 - 0.030(5)$. In the discussions below, the samples are denoted as $LnTi_{0.5}V_{0.5}O_3$ for convenience. The crystal structures were examined by

0022-4596/01 $35.00

powder XRD (X-ray diffraction) measurements using Cu$K\alpha$ radiation (MAC Science Co., M03XHF^{22}). The XRD patterns were verified to consist only of the reaction products, and were analyzed by the Rietveld method using the program RIETAN (12). Since the analyses were hardly affected if both of the actual and nominal contents were assumed for each element, only the results on the basis of the nominal contents will be shown.

DC magnetization measurements were carried out using a SQUID magnetometer (Quantum Design MPMS). DC susceptibility–temperature (χ–T) curves were measured between 4.5 and 300 K in both FC (field-cooled) and ZFC (zero-field-cooled) conditions with an applied field between 1000 and 50,000 Oe. In the former case, the measurements were carried out on cooling with the magnetic fields. Magnetization–magnetic field (M–H) curves were measured with the field within $\pm$ 55,000 Oe at 4.5 K. AC susceptibility–temperature ($\chi(\nu)$–T) curves were measured on heating the samples after the zero-field cooling down to 4.5 K. The field strength of an AC field is 4 Oe, and the frequency ν is between 0.8 and 800 Hz.

RESULTS AND DISCUSSION

Figure 1 shows the XRD patterns for $\mathrm{CeTi}_{0.5}\mathrm{V}_{0.5}\mathrm{O}_3$ and $\mathrm{PrTi}_{0.5}\mathrm{V}_{0.5}\mathrm{O}_3$. They could be fitted to the orthorhombic perovskite type *Pnma* as is the case of the end compounds (3, 8, 13), assuming the random occupation of the Ti and V ions at the same crystallographic site. The lattice parameters are shown in Table 1 together with those of the end compounds, for which the reliability (R) factors and goodness-of-fit (S) indicators were up to $\sim$18% and $\sim$1.5, respectively. The atomic positions were close to those of CeTiO_3 (3). The lattice parameters for the end compounds are close to those reported previously (3, 4, 8, 13). For $Ln\mathrm{Ti}_{0.5}\mathrm{V}_{0.5}\mathrm{O}_3$, the parameters are between those of the corresponding end compounds, suggesting that both of the Ti and V ions maintain the valence state 3 + .

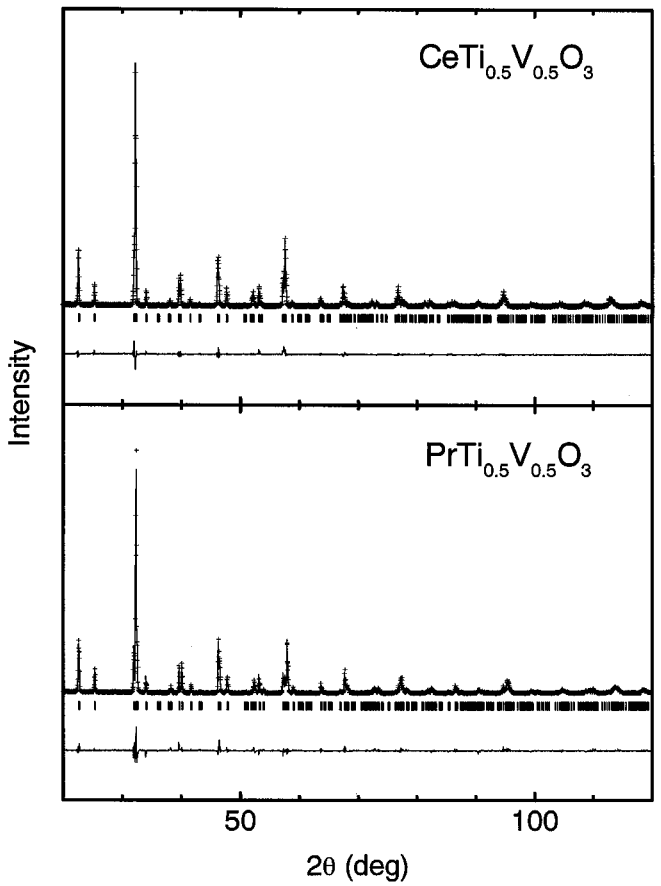

FIG. 1. XRD patterns at room temperature for $\mathrm{CeTi}_{0.5}\mathrm{V}_{0.5}\mathrm{O}_3$ and $\mathrm{PrTi}_{0.5}\mathrm{V}_{0.5}\mathrm{O}_3$ (space group *Pnma*). See Table 1 for the lattice parameters. The observed and calculated patterns are shown as the cross markers and the top solid line, respectively. The vertical markers stand for the angles of Bragg reflections. The lowest solid line represents the difference between the calculated and observed intensities. Reliability factors (R) and Goodness-of-fit (S) indicators are $R_{\mathrm{WP}} = 13.8\%$, $R_{\mathrm{I}} = 3.59\%$, $R_{\mathrm{F}} = 2.47\%$, $S = 1.37$, for $\mathrm{CeTi}_{0.5}\mathrm{V}_{0.5}\mathrm{O}_3$, and $R_{\mathrm{WP}} = 18.8\%$, $R_{\mathrm{I}} = 5.52\%$, $R_{\mathrm{F}} = 4.47\%$, $S = 1.44$ for $\mathrm{PrTi}_{0.5}\mathrm{V}_{0.5}\mathrm{O}_3$. Isotropic thermal parameters were fixed to be 0.3 Å^2.

Figures 2a and 2b show the χ–T curves for two of the end compound CeVO_3 and PrVO_3, respectively. For the FC case, the shapes of the curves, low-temperature susceptibilities, and Neel temperatures of $T_{\mathrm{N}} \sim$ 140–145 K are similar to those reported previously (8). The deviation between the FC and ZFC curves is due to the canted antiferromagnetic order at T_{N}. The inflection around 60 K might be ascribed to the order of the lanthanide moments as in $Ln\mathrm{TiO}_3$ (*Ln*: lanthanides) (3, 6). The curves of CeTiO_3 and PrTiO_3 have been reported by the authors (14, 15), which are in fair agreement with those in the previous reports (2, 5). Their canted antiferromagnetic order like that in Fig. 2 occurs at $T_{\mathrm{N}} \sim$ 120 K. Since these systems show another upturn of susceptibility at lower temperatures ($\sim$ 60–80 K) due to the order of the Ce^{3+} and Pr^{3+} moments (2, 3, 5, 6), the profiles of the curves have analogous shapes to those for CeVO_3 and PrVO_3.

Figure 3a shows the χ–T curves for $\mathrm{CeTi}_{0.5}\mathrm{V}_{0.5}\mathrm{O}_3$ with an applied field (H) of 1000 Oe. The profile of each curve is different from those of the end compounds (Fig. 2, and Refs. 2, 7, 8, 14, and 15). Rapid increases in susceptibilities are observed in both curves around $\sim$50 K, where temperature derivative of inverse susceptibility–temperature ($1/\chi$–T) curves showed maximums. Figure 3b shows an FC $1/\chi$–T curve. Above $\sim$ 170 K, the curve could be fitted with the Curie–Weiss (CW) law. The slope of the curve was found to be almost equal to the sum of the effective moment of Ce^{3+} (2.56 μ_{B} (16)), and the spin-only moments of Ti^{3+} (1.73 μ_{B}) and V^{3+} (2.83 μ_{B}) with the nominal molar contents. An

TABLE 1
Lattice Parameters for All the Systems Studied

Compoud	a(Å)	b(Å)	c(Å)
$CeTiO_3$	5.6098(1)	7.8672(2)	5.5889(1)
$CeTi_{0.5}V_{0.5}O_3$	5.5912(1)	7.8412(2)	5.5377(1)
$CeVO_3$	5.5598(1)	7.8071(2)	5.5179(1)
$PrTiO_3$	5.6347(2)	7.8294(2)	5.5614(2)
$PrTi_{0.5}V_{0.5}O_3$	5.5935(1)	7.8047(2)	5.5499(1)
$PrVO_3$	5.5739(2)	7.7719(2)	5.4826(2)

Note. The space group is commonly orthorhombic *Pnma*.

antiferromagnetic Weiss temperature ~ -135 K indicates that a dominant magnetic interaction is antiferromagnetic as in the end compounds. Thus the transition temperature will be denoted also as T_N. The temperature of $T_N \sim 50$ K is lower than those of the end compounds $\sim$120–140 K. The deviation of $1/\chi$–T curves from the CW law below $\sim$170 K is plausibly because of this magnetic transition. The second transition or inflection is found at T_{N2} of $\sim$30 K. The FC susceptibility increases again below this temperature, while the ZFC susceptibility exhibit a peak or cusp around this temperature. Therefore, both curves deviate below T_{N2}.

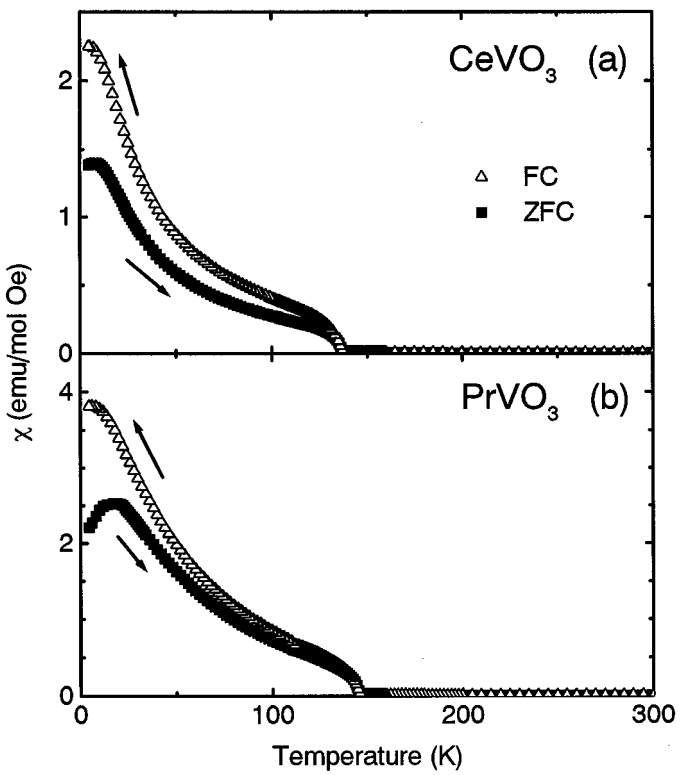

FIG. 2. χ–T curves (a) $CeVO_3$ and (b) $PrVO_3$ with an applied field of 1000 Oe. The arrows $\rightarrow$ and $\leftarrow$ represent zero-field-cooled (ZFC) and field-cooled (FC) modes, respectively.

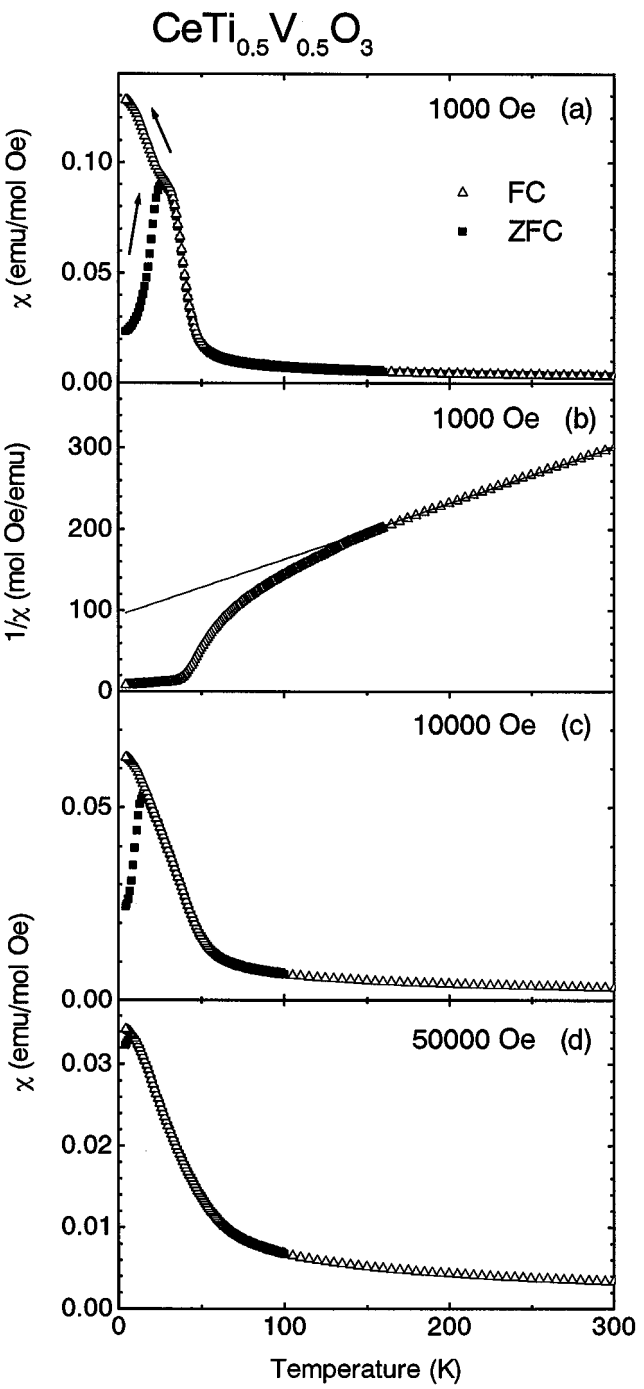

FIG. 3. (a) χ–T curves and (b) FC $1/\chi$–T curve for $CeTi_{0.5}V_{0.5}O_3$ with an applied field (H) of 1000 Oe. The solid line stands for Curie–Weiss (CW) fit. The meaning of the arrows are as in Fig. 2. (c and d) χ–T curves for H = 10,000 and 50,000 Oe, respectively.

A large hysteresis loop shown in Fig. 4 shows the existence of magnetic order at low temperatures.

Figures 3c and 3d show the χ–T curves with H = 10,000 and 50,000 Oe, respectively. The deviation between the FC

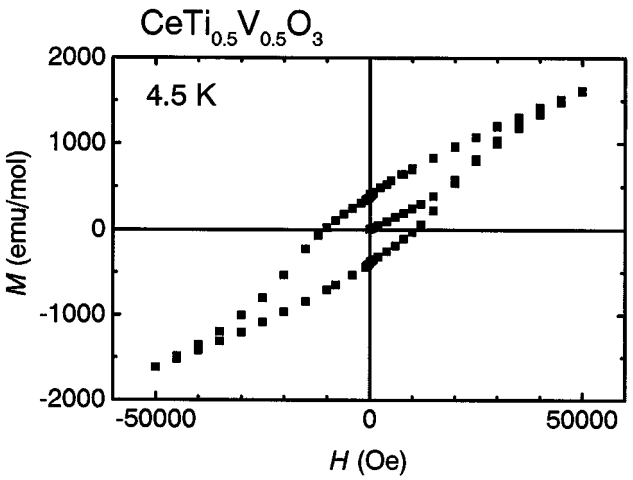

FIG. 4. M–H curve for $CeTi_{0.5}V_{0.5}O_3$ measured at 4.5 K.

and ZFC curves becomes steadily smaller with increasing H, which was confirmed also from the measurements with $H = 5000$ Oe. This trend was obtained also for the end compounds, which might be understood in terms of the rotation of magnetic domains. The deviation of both curves still remains around 5–10 K with $H = 50{,}000$ Oe. Though the transition at T_N becomes less sharp with increasing H, the curves deviate from the CW law around this temperature. The monotonic decrease in the low-temperature susceptibilities with increasing H indicates the suppression of magnetic order by the magnetic field. The value of $d(\chi H)^2/dT$ (H: applied field), corresponding to a specific heat, showed broad peaks around 15–35 K whose widths were 10–20 K.

Figure 5 shows the χ–T curves for $PrTi_{0.5}V_{0.5}O_3$. Magnetic transitions occur at $T_N \sim 50$ K, which is also a considerably lower temperature than those of the end compounds (5, 7, 8, 14). An overall trend in the figure is qualitatively the same as in $CeTi_{0.5}V_{0.5}O_3$, except that no apparent additional transition in the FC curves below T_N is observed. The deviation of the FC and ZFC curves is observed below ~ 30 K. A large hysteresis loop with coercivity $\sim 11{,}000$ Oe was obtained at 4.5 K. The localized moment obtained from the CW fit was close to the sum of the effective moment of Pr^{3+} (3.62 μ_B (16)) and the spin-only moments of Ti^{3+} and V^{3+} as in $CeTi_{0.5}V_{0.5}O_3$. The Weiss temperature was also antiferromagnetic, ~ -75 K.

The peak or cusp in the ZFC curves, and the deviation between the FC and ZFC curves noted above can be observed also for the canted-antiferromagnetic order as reported for $SmTiO_3$ (9). However, considering that the transition temperatures are drastically lowered down to ~ 30–50 K, entire alternation of the magnetic order plausibly occurs in the present systems. It is noteworthy that the phenomena obtained here are characteristic also of spin-glass (and spin-glass-like systems) and superparamagnetism (17–23). The suppression of magnetic order by increasing H (Figs. 3 and 5) and the magnetic hysteresis (Fig. 4) are consistent with this speculation (17, 18, 23). The broad peaks of $d(\chi H)^2/dT$ noted earlier might indicate also the existence of such states (17).

Figure 6 shows magnetization at 6 K measured against time for $CeTi_{0.5}V_{0.5}O_3$. The sample was cooled with $H = 100$ Oe down to 6 K. Then the measurement was started immediately after reducing the field to zero. It is found that the magnetization shows nonexponential logarithmic time dependence. This type of relaxation is another characteristic of spin-glass and superparamagnetism (17-19).

Figure 7 show $\chi(\nu)$–T curves for $CeTi_{0.5}V_{0.5}O_3$ with several AC frequencies ν. Figure 7a shows that the real part (χ') of $\chi(\nu)$ has the maximum at $T' \sim 33$–35 K. No apparent peak has been observed below and above this temperature.

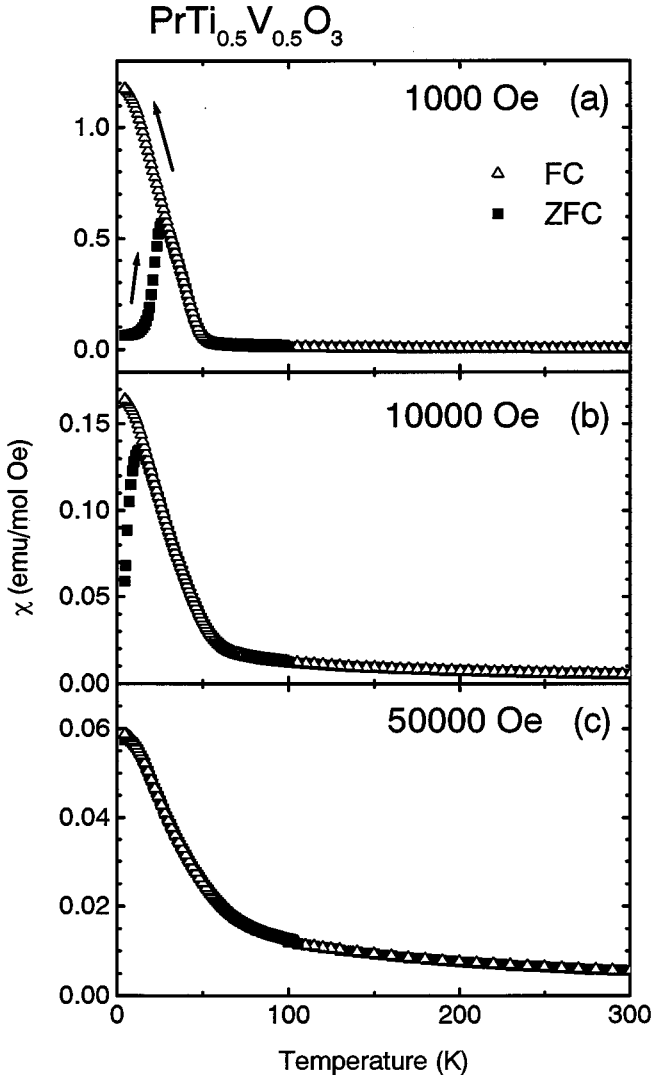

FIG. 5. χ–T curves for $PrTi_{0.5}V_{0.5}O_3$ with an applied field (H) of (a) 1000 Oe, (b) 10,000 Oe and (c) 50,000 Oe. The meaning of the arrows are as in Fig. 2.

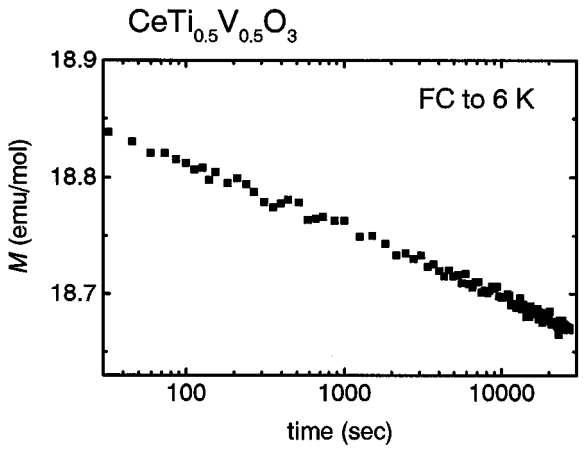

FIG. 6. Magnetization (M) plotted against time, measured at 6 K for $CeTi_{0.5}V_{0.5}O_3$.

This means that the deviation from the CW fit below $\sim$170 K is because of the onset of magnetic correlation (18). It is clear that the value of T' is dependent of v, i.e., T' becomes higher with increasing v. To distinguish spin-glass and superparamagnetism, the frequency dependence of T' given as $\Delta T'/[T'\Delta \log v]$ has been regarded as an empirical criterion, where $\Delta T'$ and $\Delta \log v$ are the shifts of T' and $\log v$, respectively (18, 20). Usually this value is $\sim$0.01 for spin-glass, but larger than 0.1 for superparamagnetism. For the present system, this value was calculated to be $\sim$0.02. Thus, it is considered that the present magnetic behavior is caused by a spin-glass.

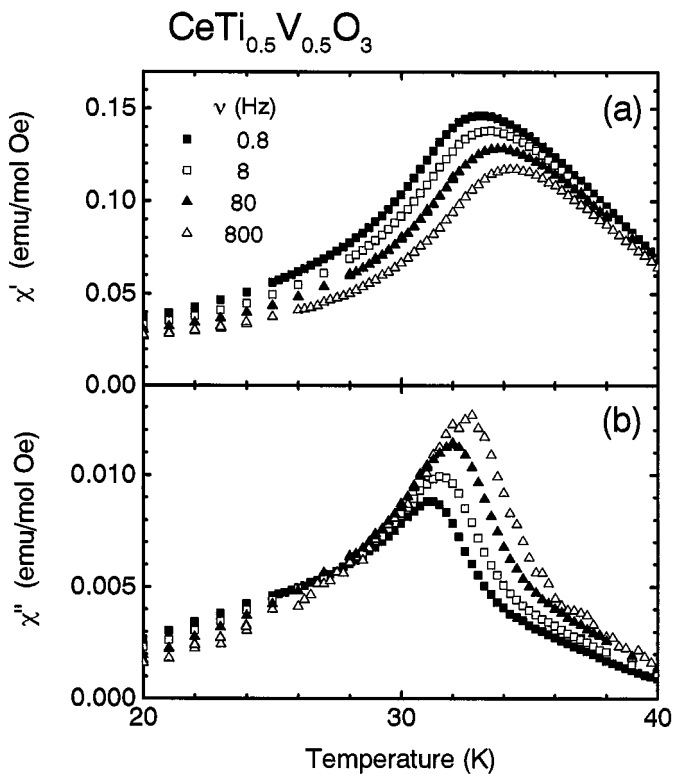

FIG. 7. $\chi(v)$–T curves for $CeTi_{0.5}V_{0.5}O_3$ with several AC frequencies v. χ' and χ'' stand for real and imaginary parts of $\chi(v)$, respectively.

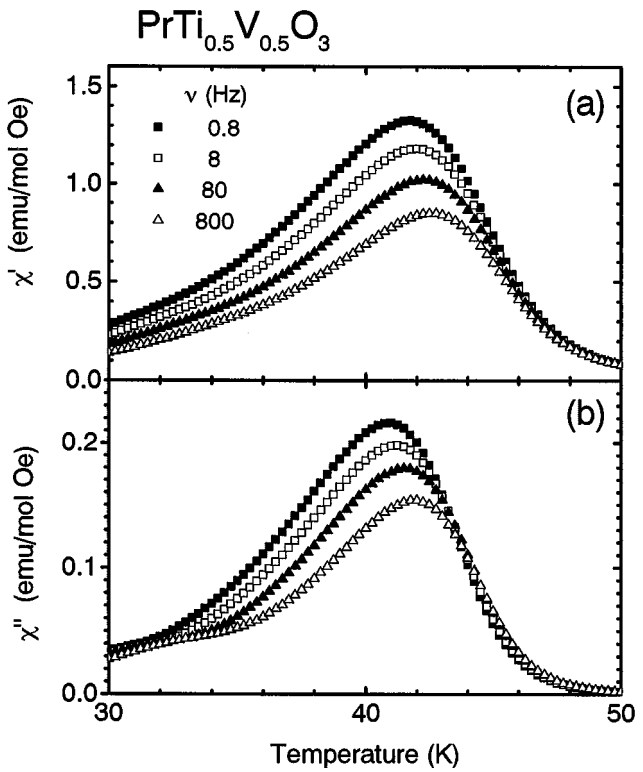

FIG. 8. $\chi(v)$–T curves for $PrTi_{0.5}V_{0.5}O_3$ with several frequencies v.

Figure 7b shows that also the imaginary part (χ'') of $\chi(v)$ has the maximums at $T'' \sim 31$–33 K. The maximums indicate the emergence of irreversibility around T'', due to the spin-glass formation. The values of T' and T'' for each frequency are slightly different by $\sim$1 K. The value of T'' increases with increasing v as is true also for T', which have been reported for other spin-glasses such as $Eu_{0.2}Sr_{0.8}S$ (22) and $Cr_2Sn_3Se_7$ (18). The phenomena observed here, i.e., both T' and T'' are frequency dependent, and are not coincident to each other, are regarded as the exact criteria of spin-glass behavior (21). Essentially, identical frequency dependence has been obtained also for $PrTi_{0.5}V_{0.5}O_3$, whose $\chi(v)$–T curves are shown in Fig. 8.

One possible origin for the spin-glass formation is the magnetic frustration due to the coexistence of a competition between ferromagnetic and antiferromagnetic interactions, and the random spatial distribution of both interactions. The lower transition temperatures than those in the end compounds plausibly imply the suppression of long-range magnetic order, caused probably by magnetic frustrations. This speculation is consistent with the existence of spin-glasses. The random occupation of the Ti and V ions is obviously one origin for the spin-glass. The Ti^{3+}–Ti^{3+} ($3d^1$)

and V^{3+}–V^{3+} ($3d^2$) interactions are expected to be antiferromagnetic, judging from the situation in the end compounds (1, 2, 4, 5, 8), where such interactions are assumed to arise from the quenched 3*d* orbitals. Due to the Hund's rule, ferromagnetic interactions can arise if the 3*d* electrons move into any empty 3*d* orbitals even if the orbitals are quenched. The present results suggests this situation, which might be realized by slight differences of energies and electronic states between the Ti3*d* and V3*d* orbitals. For further discussion, determination of the electronic states is to be done, based on the measurements such as photoemission or X-ray absorption spectroscopy.

To obtain more information on magnetic properties, the investigations for the $Ln\mathrm{Ti}_{1-x}\mathrm{V}_x\mathrm{O}_3$ compounds with x other than 0.5 are now in progress. The lattice parameters for $\sim 0.1 < x < \sim 0.8$ with the x step of 0.1–0.2 were found to change almost continuously and monotonically with increasing x, indicating the formation of solid solutions. Their results on magnetic properties will be published in the future.

In summary, the crystal structures of $Ln\mathrm{Ti}_{0.5}\mathrm{V}_{0.5}\mathrm{O}_3$ (Ln = Ce and Pr) are an orthorhombic perovskite type (*Pnma*), where the Ti and V ions are settled with random occupation at the same crystallographic site. From the measurements of χ–T curves, magnetization relaxation, and $\chi(v)$–T curves, it was suggested that spin-glasses are formed at low temperatures arising from the random occupation of the Ti and V ions.

REFERENCES

1. J. E. Greedan, *J. Less-Common Metals* **111,** 335 (1985).
2. D. A. MacLean and J. E. Greedan, *Inorg. Chem.* **20,** 1025 (1981).
3. J. P. Goral and J. E. Greedan, *J. Magn. Magn. Mater.* **37,** 315 (1983).
4. J. E. Sunstrom IV, S. M. Kauzlarich, and M. R. Antonio, *Chem. Mater.* **5,** 182 (1993).
5. D. A. MacLean, K. Seto, and J. E. Greedan, *J. Solid State Chem.* **40,** 241 (1981).
6. J. E. Greedan, *J. Magn. Magn. Mater.* **44,** 299 (1984).
7. T. Katsufuji, Y. Taguchi, and Y. Tokura, *Phys. Rev. B* **56,** 10145 (1997).
8. H. C. Nguyen and J. B. Goodenough, *J. Solid State Chem.* **119,** 24 (1995).
9. G. Amow, J. E. Greedan, and C. Ritter, *J. Solid State Chem.* **141,** 262 (1998), doi:10.1006/jssc.1998.7989.
10. J. B. Goodenough and J. M. Longo, "Landolt-Bornstein," Group III, Vol. 4. Springer-Verlag, New York, 1970.
11. S. Nomura, "Landolt-Bornstein," Group III, Vol. 12. Springer-Verlag, New York, 1978.
12. F. Izumi, *in* "The Rietveld Method" (R. A. Young, Ed.), Chap. 13. Oxford Univ. Press, Oxford, 1993; Y.-I. Kim and F. Izumi, *J. Ceram. Soc. Jpn.* **102,** 401 (1994).
13. JCPDS card, 29–1075.
14. K. Yoshii and A. Nakamura, *J. Solid State Chem.* **137,** 181 (1998), doi:10.1006/jssc.1998.7824.
15. K, Yoshii, A. Nakamura, H. Abe, and Y. Morii, *J. Solid State Chem.* **153,** 145 (2000), doi:10.1006/jssc2000.8765.
16. J. H. Van Vleck, "The Theory of Electric and Magnetic Susceptibilities." Oxford Univ. Press, London, 1965.
17. K. Binder and A. P. Young, *Rev. Mod. Phys.* **58,** 801 (1986).
18. F. Bodénan, V. B. Cajipe, M. Danot, and G. Ouvard, *J. Solid State Chem.* **137,** 249 (1998), doi:10.1006/jssc.1997.7723.
19. H. Mamiya, I. Nakatani, and T. Furubayashi, *Phys. Rev. Lett.* **80,** 177 (1998).
20. J. A. Mydosh, *in* "Spin Glasses," p. 66. Taylor and Francis, London, 1993.
21. S. L. Suib and L. E. Iton, *Chem. Mater.* **6,** 429 (1994).
22. D. Huser, L. E. Wenger, A. J. van Duyneveldt, and J. A. Mydosh, *Phys. Rev. B* **27,** 3100 (1983).
23. H. Aruga, A. Ito, H. Wakabayashi, and T. Goto, *Physica B* **155,** 311 (1989).